INTERPRETING SENTINEL-1 RADAR BACKSCATTERING FOR THE MELT DYNAMIC OF AN ALPINE SNOWPACK WITH A HIGH RESOLUTION GROUND TRUTH DATASET

Francesca Carletti[1,*], Carlo Marin[2], Mathias Bavay[1], Michael Lehning[1,3]

[1] *WSL Institute for Snow and Avalanche Research SLF, Davos, Switzerland*
[2] *Institute for Earth Observation, Eurac Research, Bolzano, Italy*
[3] *School of Architecture, Civil and Environmental Engineering, École Polytechnique Fédérale de Lausanne EPFL, Lausanne, Switzerland*

ABSTRACT: Snow in mountain catchments serves as a constant water release during the melting season, supporting many human activities downstream. However, it also poses threats to human life and infrastructures, e.g. with wet- or glide-snow avalanches. These avalanches are likely to occur more frequently with a warming climate but are hard to predict due to the spatio-temporal complexity of the involved processes. The snow liquid water content is a key parameter to monitor to address both potentialities and challenges of a melting snowpack. Synthetic Aperture Radar products like Sentinel-1 are valid tools for detecting wet snow, as liquid water increases dielectric losses absorption coefficients, resulting in low backscattering values. Although energy-balance snow models can simulate liquid water distribution as well as other scattering properties, continuous ground truth measurements are needed for validation. However, such datasets are rare, because they are very demanding as of resources and expertise. We present part of a comprehensive dataset of full snow profiles covering one snow season at the Weissfluhjoch field site (Switzerland). This dataset includes detailed manual measurements of important snow microwave properties: temperature, density, specific surface area, liquid water content, and surface roughness. The high temporal and vertical resolution of the dataset allowed us to track the evolution of the wetting front in detail. Moreover, making use of the Snow Microwave Radiative Transfer model (SMRT), we were able to use ground data to successfully reproduce the Sentinel-1 backscattering. Finally, we could give a detailed explanation of the physical processes driving Sentinel-1 backscattering trends and explore the potential of interpreting these trends to track the melting snow process.

Keywords: Snowmelt, SAR, Sentinel-1, liquid water content, surface roughness, snow profiles

1. INTRODUCTION

Snow in mountain catchments is an important water resource, accumulating and storing water during winter and releasing it consistently during the melting season (Viviroli and Weingartner, 2004). This reliable release from higher altitudes supports many human activities downstream, including agriculture and hydropower production (Beniston et al., 2018). At the same time, snow poses significant threats to human life and infrastructures during the melting season, such as wet-snow or glide-snow avalanches. Despite their likely increasing occurrence due to a warming climate, predicting these avalanches remains challenging due to the spatiotemporal complexity of the involved processes. The presence and distribution of liquid water content (LWC) within the snowpack is a key parameter to monitor in order to address the above mentioned challenges and potentialities, as it is one of the drivers of glide-snow avalanche formation and it can well identify the different stages of the melting season. Multilayer, energy-balance snow models can in principle simulate the distribution of LWC and other key snow properties at high resolution in time and space. However, performances heavily depend on the quality of the input data, the chosen parametrizations and the structure of the models. On the other hand, Synthetic Aperture Radar (SAR) images have proven useful for wet snow detection: as the free liquid water in snow increases, dielectric losses and, consequently, absorption coefficients rise (Ulaby et al., 2014). As a result, the average backscattering experiences a significant drop when the snow starts wetting (Mätzler, 1987; Shi and Dozier, 1992; Nagler et al., 2016; Marin et al., 2020; Naderpour et al., 2021). However, the LWC in the snowpack only partially explains the behaviour of the coefficient of backscattering, as the latter is also affected by other scattering properties, such as surface roughness, density, the specific surface area (SSA) and potentially the large structures buried underneath a wet snowpack such as ice lenses or pipes (Shi and Dozier, 1995). Some of these properties can be simulated by snow models at a high input data quality and computational cost (Wever et al., 2014, 2016), but the validation of the outputs is challenging, because

*Corresponding author address:
Francesca Carletti, WSL Institute for Snow and Avalanche Research SLF
Flüelastrasse 11, 7260 Davos Dorf, Switzerland;
tel: +41 81 4170 162
email: francesca.carletti@slf.ch

the snowpack properties should be sampled at a high vertical resolution and continuously over time. Such datasets are rare, because their collection is time intensive and requires expertise. In this work, we present a portion of a comprehensive dataset made of full snow profiles collected over one snow season over the field site of Weissfluhjoch, Davos, Switzerland. This dataset includes detailed manual measurements of important snow properties, many of which affect the scattering: temperature, density, specific surface area, liquid water content and surface roughness. The snow properties were sampled with a high vertical resolution, weekly during the dry season and up to three times per week during the melting season until complete snow ablation. We use the manually measured snow properties to validate the SNOWPACK model (Bartelt and Lehning, 2002) and to reproduce Sentinel-1 backscattering making use of the Snow Microwave Radiative Transfer model (Picard et al., 2018). Since its release, this model has been widely used to reproduce backscattering and brightness temperature over Artic and Antarctic snowpack (Picard et al., 2022b; Fan et al., 2023) and on lake ice (Murfitt et al., 2022). This work aims at explaining the physical processes driving Sentinel-1 backscattering trends and exploring the potential of interpreting these trends to track the melting snow processes.

2. STUDY SITE, DATA, MEASUREMENTS AND MODELS

2.1 Study site: Weissfluhjoch Versuchsfeld

The measurement campaign was conducted at Weissfluhjoch Versuchsfeld (WFJV), Davos, Grisons, Switzerland. This reference field site lies at an altitude of 2536 m a.s.l., on a flat area embedded in a valley facing south-east. It is easily accessible, protected from avalanche danger and provides shelter for instruments and workers. This site is equipped with advanced meteorological sensors, and has one of the longest recorded time series of snow measurements for a high-altitude research station.

2.2 The snow season of 2022-2023

The snow profiles presented in this paper were sampled in the 2022-2023 snow season, starting on 14/02 and ending on 16/06, 2023. This snow season was especially dry, snowfalls were not abundant, isolated, and followed by long dry periods. In March 2023 a snow height of 107 cm was measured, matching the lowest measured snow height on record for this day of the year. Generally, measured snow heights were very close to the recorded minima. Temperatures fluctuated between well above zero and freezing values between December and March, giving rise to frequent superficial melt events. These conditions favoured the early formation of ice lenses, i.e. horizontal ice layers formed as a consequence of water percolating the snowpack, hitting colder or denser layers, expanding horizontally and refreezing. Temperature then dropped again in late spring when isolated snowfalls were recorded.

2.3 Measurements

The temperature was sampled every 10 cm using a thermometer (specified for a 0.2 ℃ accuracy and in practise accurate at 0.1 ℃). The LWC was sampled every 2 cm using the Denothmeter (Denoth, 1994). The density was sampled every 3 cm using a snow cutter (Proksch et al., 2016). The SSA was sampled every 4 cm using the InfraSnow sensor (FPGA Company). Finally, the surface roughness was measured with a digital photography based approach (Barella et al., 2021).

2.4 Sentinel-1 satellite data

Sentinel-1 (S1) is a two-satellite constellation with a revisit time of 6 days acquiring SAR images in the C-band in dual polarization at the frequency of 5.405 GHz. Because of the swath width and the cycle length of 175 orbits, at the Alpine mid-latitudes normally more than one acquisition every 6 days is available. For WFJV, four tracks are available with a resolution of 5 x 20 m at vertical and mixed polarization. Throughout the measurement campaign, the S1 data availability has an average of one image every 2.5 days and a mode of one every 3 days. The images can be downloaded for free from the Copernicus data hub (Copernicus). The resulting backscattering time series are the result of a series of processing steps described in Marin et al. (2020).

2.5 Models

The quality of the forcing data recorded at WFJV allowed to produce a high-resolution 1D snow simulation over the 2022-2023 snow season using the energy-balance, layer based model SNOWPACK (Bartelt and Lehning, 2002; Wever et al., 2014, 2016). In order to reproduce the ice layers build up in the snow pack during the melt season, the Richards equation solver has been used (Wever et al., 2014) as well as the dual-domain approach to simulate preferential flow (Wever et al., 2016) and the ice reservoir approach to allow the refreeze of the ponding resulting from preferential flow (Quéno et al., 2020). To reproduce S1 backscattering, the field data was cleaned, homogenized and resampled to a common vertical resolution of 6 cm, comparable to the wavelength of S1. The time series of snow properties per layer is then fed to the Snow Microwave Radiative Transfer model (SMRT), a model built to perform simulations of microwave response from snowpacks, fully described in Picard

et al. (2018). The user has to specify a microstructure, electromagnetic and permittivity model and the model solves the radiative transfer equations to generate a time series of backscattering intensities. In this study, we used the exponential model with polydispersity equal to 0.6 (Picard et al., 2022b) to describe the microstructure, the integral equation model (IEM) for surface scattering (Brogioni et al., 2010) and, the symmetrized strong-contrast expansion (SymSCE) (Picard et al., 2022a) as the electromagnetic model with the semi-empirical permittivity model developed by Sihvola (2000). At present, this combination is among the optimal ones to describe wet snow starting from measured variables, however additional research is still necessary.

3. RESULTS

3.1 Field measurements and SNOWPACK simulation

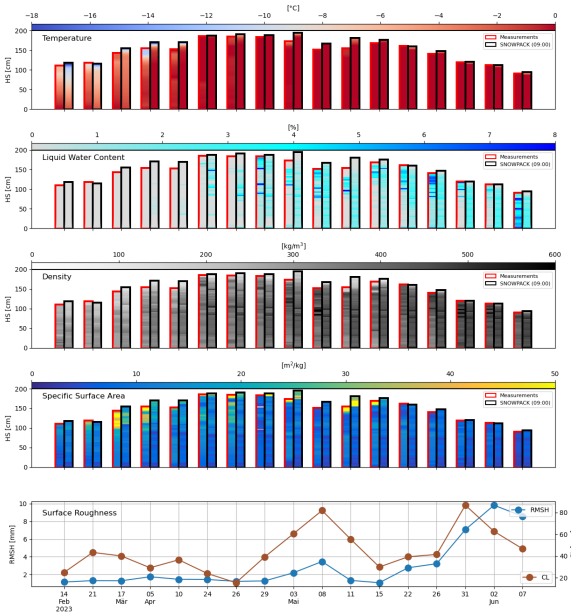

Figure 1: Overview of the selection of snow profiles from the 2022-2023 campaign, measured (red outline) and modelled with SNOWPACK (black outline). From top to bottom: snow temperature, LWC, density, SSA and surface roughness expressed as root mean square of the heights (blue) and correlation length (brown).

Figure 1 shows a selection of the snow profiles, modelled with SNOWPACK and sampled during the measurement campaign: snow height, temperature, LWC, density, SSA and surface roughness. These are the main parameters influencing the scattering phenomena for snow, and therefore the necessary inputs for the radiative transfer model. As is to be expected, the measured and modelled snow heights differ, sometimes quite significantly. We decided not to correct these discrepancies because it would imply modifying the measured snow properties in a non-obvious manner. Measurements show that the snowpack reached the full isothermal state on 29/04, 5 days later than the model prediction. In general, the modelled transition from frozen to isothermal is more abrupt than it was observed in the field. The first significant surface melt event was measured on 29/04. From this date on, measurements show that the surface LWC progressively increases (or resets to zero as a consequence of refreezing or spring snowfalls) ponding above the thick ice lens that formed at around 100 cm from the ground. As the snowmelt progresses and as the ice lens disintegrates, the LWC distribution starts being more homogeneous until the end of the campaign. Conversely, the simulation exhibits an earlier start of the melt, almost 20 days earlier than observed in the field. This melt is followed by ponding that holds LWC above an ice layer for more than a week (24/04 until 03/05). Then, the LWC breaks through and although there is still some ponding visible at various depths, this does not prevent the flow of LWC all the way through the snowpack. In the measurements, the wetting starts much later and the ponding over the ice layer holds for much longer (29/04 until 26/05) before significant amounts of LWC can bee seen below. Therefore, although the model succeeds in representing complicated preferential schemes like ice layers and ponding, these phenomena verified in a much enhanced way in the field, leading to very different snowpack conditions with respect to the model predictions. This is confirmed by both density and SSA. High LWC or ice layers are characterized by high densities and lower SSAs. Dry, drained, or new snowfall layers have low densities and high SSAs. Lastly, the measurements of snow surface roughness were translated into the root mean square of the heights (RMSH) and the correlation length (CL), which are used in the definition of the exponential autocorrelation function used by the IEM. RMSH and CL describe roughness in a different way, however in practice, the RMSH is generally low for smooth surface and increases with the development of surface macroscopic roughness formation like suncups in the later stage of the melting season – being a self organized process which generates a quasi-periodic pattern (Betterton, 2001; Herzfeld et al., 2003), also the CL is generally increasing.

3.2 SMRT simulations and Sentinel-1

In Figure 2, we show the results of the simulated backscattering from measured and modelled snow profiles using the model SMRT, along with the recorded S1 backscattering values. As a consequence of the earlier wetting simulated by SNOWPACK, the backscattering drop of 3 dB lower than the winter mean is generated 6 days earlier than recorded by the SAR (respectively, on 23/04 and on 29/04). The simulation performed using SNOWPACK snow profiles shows an isolated melt event at

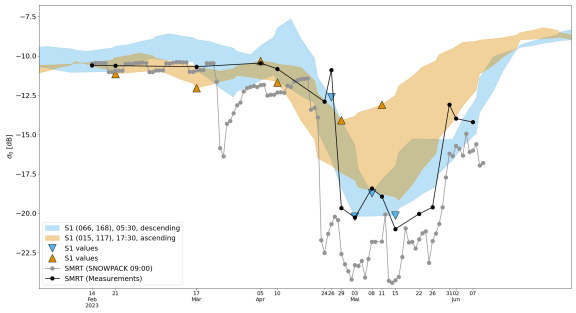

Figure 2: S1 morning (light blue area) and afternoon (orange area) recorded backscattering; together with the backscattering time series simulated with SMRT using ground measurements (black line) and SNOWPACK simulation (grey line) inputs. S1 values recorded on the same day as manual measurements are reported as triangles, light blue for morning passes and orange for afternoon passes.

the end of March that was missed by the measurement campaign. However, a backscattering drop of 2.5 dB is also recorded over that period by the morning satellite passes. In general, there seems to be a negative bias in the SNOWPACK generated backscattering time series since the first isolated melt event. The backscattering simulated using the measured snow profiles reproduces well the S1 trends, both in terms of wetting timing and lowest values. On days when manual measurements and satellite passes coincide, the Mean Bias Error and the Root Mean Square Error are equal to respectively 3.9 and 5.0 dB for the backscattering generated with SNOWPACK and 1.7 and 2.7 dB for the backscattering generated with manual measurements.

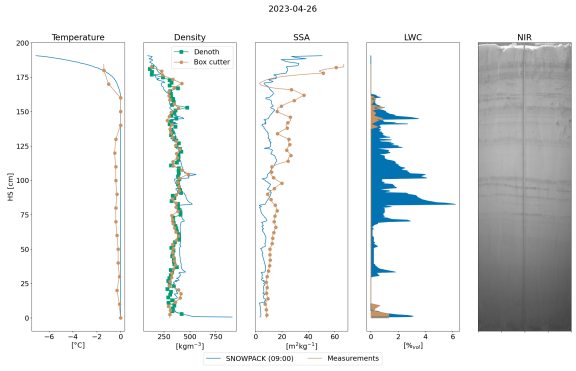

Figure 3: Detailed snow properties measured (brown) and modelled with SNOWPACK (blue) on April 26th. From left to right: temperature, density (the additional green line represents the dry snow density measured with the Denoth), SSA, LWC and a Near-Infra-Red picture qualitatively highlighting wet layers over dry ones.

The snowpack properties that cause the time lag in the generated backscattering drop between SNOWPACK and manual measurements can be better understood comparing the modelled and observed snow profiles on 26/04 (Figure 3) and on 03/05 (Figure 4), when the backscattering drops take place for SNOWPACK respectively for the measurements. On 26/04, SNOWPACK models a colder snow surface with respect to measurements, and an otherwise isothermal snowpack; measurements only show an isothermal layer below the frozen surface and otherwise a snowpack that is still frozen. Measured and modelled densities are in overall agreement, although modelled densities from the ground up to 125 cm seem slightly overestimated. SSA is underestimated by the model over the whole snowpack. The modelled LWC is distributed over the whole snowpack below the frozen surface with an average value of 0.85%, in accordance with higher densities and lower SSA. On the field, LWC was only measured between 160 and 140 cm from the ground and at the ground level with a maximum value of around 1%. The NIR image qualitatively confirms the measured snow properties, showing a profile that is still relatively dry, where several ice lenses formed, obstructing free water from flowing in lower sections. On 03/05, the day where the minimum value of morning backscattering was recorded by S1, the modelled temperature, density and SSA remain rather unchanged. The measured profile is isothermal below the frozen surface, thus theoretically allowing the formation of liquid water in the snowpack. However, the wetting front has not progressed much with respect to 26/04 likely due to the presence of an ice lense at 105 cm from the ground, also visible in the NIR image. Above this ice lense, the volumetric LWC more than doubled reaching a value of around 7.5% before being blocked from flowing downwards. The modelled LWC is distributed more homogeneously over the snowpack but has higher average value (1.2%) with respect to measurements (0.8%), explaining the lower backscattering generated from SMRT with this input.

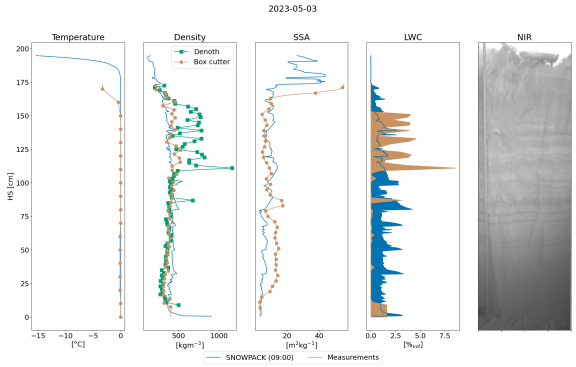

Figure 4: Detailed snow properties measured (brown) and modelled with SNOWPACK (blue) on May 3rd. From left to right: temperature, density (the additional green line represents the dry snow density measured with the Denoth), SSA, LWC and a Near-Infra-Red picture qualitatively highlighting wet layers over dry ones.

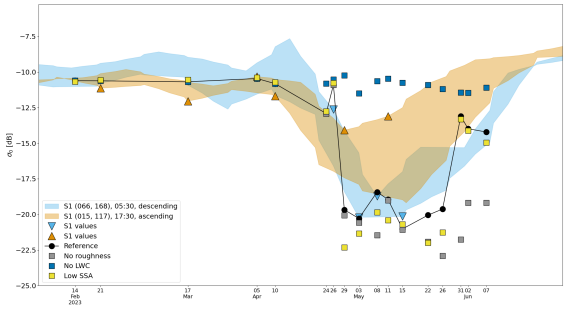

Figure 5: S1 morning (light blue area) and afternoon (orange area) recorded backscattering; together with the backscattering time series simulated with SMRT using ground measurements (black line) as a reference. S1 values recorded on the same day as manual measurements are reported as triangles, light blue for morning passes and orange for afternoon passes. Squares represent the SMRT simulation results of the sensitivity analysis: grey squares represent the variation without surface roughness, blue squares represent the variation without LWC, yellow squares represent the variation with a constant value of SSA typical of the advanced melting period and equal to 8.1 $m^2 kg^{-1}$.

The increase in S1 backscattering that is recorded after the local minimum value happens in conjunction with three different processes within and at the surface of the snowpack (Figure 1): an increase in surface roughness due to the slow development of suncups, a potential decrease of LWC of the superficial layers due to runoff, and a decrease of surface SSA because of grain size growth during the melt process. Figure 5 shows once again the simulated backscattering from the field data, this time with three variations, to explore the isolated effect of the three above mentioned mechanisms alone in SMRT. For the first variation, the roughness component was disabled in SMRT. For the second variation, LWC was set to zero at each layer of each input snow profile. For the third variation, the SSA of each layer of each snow profile was set to the average value measured from 22/05 onwards (8.1 $m^2 kg^{-1}$), in order to eliminate the effect of higher surface scattering due to smaller grains. Results in Figure 5 show that all these variations have no effect during the dry season, but as soon as the snowpack starts wetting, different processes become more or less relevant at different melting stages. Comparing the reference simulation obtained with measured snow profiles, it becomes clear that the main mechanism driving the backscattering drop from the winter mean to the local minimum value is the presence of the LWC in the snowpack, with residual effect of scattering increase when SSA is high at the surface because of refreezing or new snowfalls. S1 is also very sensitive to low values of surface roughness: on 08/05, the surface roughness caused a backscattering increase of 3 dB, even with an increase of LWC, before the snowfall flattened the surface. In general, a small increase in surface roughness generates a very quick response in backscattering increase.

4. DISCUSSION

The high resolution ground truth dataset presented in Figure 1 consists of a time series of snow profiles where the major snow scattering properties were sampled with high temporal and vertical resolution. These properties, except for surface roughness, can be generally well reproduced by physically-based snow models, if detailed and complete input data is available. However, some snowpack features like ice lenses and ponding are very hard to reproduce exactly as observed in the field, and the reason can be issues in the input data and/or in the model, spatial heterogeneity of the above mentioned processes, or a combination of these factors. Making use of the high quality observational time series, we were able to qualitatively reproduce the measured vertical snow profiles with the model SNOWPACK. However, the modelled snowpack gets to the isothermal state earlier and more abruptly than it was observed in the field: this allows LWC to start forming in the snowpack earlier with respect to measurements. Moreover, despite the model's ability to reproduce ice lenses and ponding, to simulate these processes at the same depth and timing as observed in the field remains very challenging because they depend strongly on snowpack parameters and they have great spatial variability. Using the measured and modelled snow properties, a backscattering time series was generated with the SMRT model, the results are reported in Figure 2 and compared against the recorded backscattering from S1. The backscattering time series obtained with the ground measurements generally well reproduces the trend of S1, proving that SAR systems at the C-band like S1 could be used to monitor the evolution of a melting snowpack. Only two values were severely underestimated with both the measured and modelled profile data: however, these two values belong to the same track that has a very low incidence angle. This track generates a higher spread of the afternoon backscattering values with respect to the morning ones (Figure 2). At such low incidence angles, the SAR signal may be sensitive to specific snowpack properties that need to be further investigated. Comparing the measured snow profiles on 26/04 (Figure 3) and 03/05 (Figure 4), and the recorded backscattering values in those dates (respectively -12.6 and -20.2 dB), it becomes clear that the S1 signal is experiencing losses because of the LWC increase in this time interval. As a consequence of the early presence of LWC in the modelled snow profile time series, its quantity and distribution, not only the same backscattering drop happens one week earlier, but it also shows a negative bias of approximately -2.5 dB with respect to S1 recordings. These findings are supported by the

sensitivity analysis presented in Figure 5. Here, we took the reference backscattering time series simulated by SMRT and added three variations to investigate the effect of different scattering properties isolated one from another. This analysis brought to light that the main backscattering drop in morning and afternoon tracks is mostly relatable to the progressive wetting of the snowpack, although high values of SSA at the surface (due to refreezing or new snowfalls) may increase the scattering generating a higher value of backscattering. But mainly, it is clear that the rise in backscattering after the local minimum value is mostly caused by the increase in surface roughness, with the changes in LWC becoming less impacting. By comparing the reference backscattering time series with the points describing the variation without roughness, it is interesting to notice that despite the LWC increase in the superficial layers of the snowpack between 15 and 26/05, the simulated backscattering increases in the reference simulation and keeps decreasing in the variation with no roughness. By looking at the date of 08/05, when the first remarkable roughness increase was measured, the value recorded by S1 is almost perfectly reproduced by the reference simulation, but underestimated by 3 dB when neglecting the roughness. This suggests that the backscattering from S1 has a high sensitivity to relatively low roughness values.

5. CONCLUSIONS

In this work, we presented part of a unique dataset of snow scattering properties measured at high resolution over a recent snow season at the field site of Weissfluhjoch, Davos, Switzerland and used this dataset to give an overview on how S1 backscattering can be explained by measured snow properties, with a focus on wet snow. By comparing ground data with a high quality physically based simulation, we pointed out key differences in wetting timing and liquid water release mechanisms, therefore highlighting the processes that must be better modeled for highly detailed simulation of the melt phases. By using a microwave radiative transfer model for snow, we were able to use our ground reference dataset to reproduce the S1 backscattering time series over the rather complex structure of an Alpine snowpack. This allowed to better understand the key mechanisms influencing the backscattering trends and which properties have the major influence in different stages of the melting season. We highlighted the key factors to consider in order to be able to rely on snow cover simulations to reproduce the backscattering signal recorded by S1. By conducting a sensitivity analysis, we highlighted that the presence of LWC in the snowpack is the key factor influencing the major backscattering drop from the winter average, and that at this stage there is a minor influence of high values of SSA at the surface that may cause more scattering and contrast the absorption. Once some relatively small roughness starts to develop, the surface scattering dominates the backscattering signal even against increasing LWC values. This study expands our knowledge of the complex processes within an Alpine snowpack necessary to understand trends in satellite observations and potentially use them as information to snow models in the future.

References

Barella, R., Marin, C., Mattia, C., Gianinetto, M., Moranduzzo, T., and Notarnicola, C.: A Low-Cost Portable Automatic System for Snow Surface Roughness Measurements Based on Digital Photography, pp. 5562–5565, doi:10.1109/IGARSS47720.2021.9553989, 2021.

Bartelt, P. and Lehning, M.: A physical SNOWPACK model for the Swiss avalanche warning: Part I: numerical model, Cold Regions Science and Technology, 35, 123–145, doi:10.1016/S0165-232X(02)00074-5, 2002.

Beniston, M., Farinotti, D., Stoffel, M., Andreassen, L. M., Coppola, E., Eckert, N., Fantini, A., Giacona, F., Hauck, C., Huss, M., Huwald, H., Lehning, M., López-Moreno, J.-I., Magnusson, J., Marty, C., Morán-Tejéda, E., Morin, S., Naaim, M., Provenzale, A., Rabatel, A., Six, D., Stötter, J., Strasser, U., Terzago, S., and Vincent, C.: The European mountain cryosphere: a review of its current state, trends, and future challenges, The Cryosphere, 12, 759–794, doi:10.5194/tc-12-759-2018, URL https://tc.copernicus.org/articles/12/759/2018/, 2018.

Betterton, M. D.: Theory of structure formation in snowfields motivated by penitentes, suncups, and dirt cones, Phys. Rev. E, 63, 056 129, doi:10.1103/PhysRevE.63.056129, URL https://link.aps.org/doi/10.1103/PhysRevE.63.056129, 2001.

Brogioni, M., Pettinato, S., Macelloni, G., Paloscia, S., Pampaloni, P., Pierdicca, N., and Ticconi, F.: Sensitivity of bistatic scattering to soil moisture and surface roughness of bare soils, International Journal of Remote Sensing, 31, 4227–4255, doi:10.1080/01431160903232808, 2010.

Copernicus: Copernicus data hub, URL https://scihub.copernicus.eu/.

Denoth, A.: An electronic device for long-term snow wetness recording, Annals of Glaciology, 19, 104–106, doi:10.3189/S0260305500011058, 1994.

Fan, Y., Li, L., Chen, H., and Guan, L.: Evaluation and Application of SMRT Model for L-Band Brightness Temperature Simulation in Arctic Sea Ice, Remote Sensing, 15, doi:10.3390/rs15153889, URL https://www.mdpi.com/2072-4292/15/15/3889, 2023.

FPGA Company: SLF Snow Sensor, URL https://fpga-company.com/wp-content/uploads/2023/01/InfraSnow-User-Manual-Version-1.01.pdf.

Herzfeld, U. C., Mayer, H., Caine, N., Losleben, M., and Erbrecht, T.: Morphogenesis of typical winter and summer snow surface patterns in a continental alpine environment, Hydrological Processes, 17, 619–649, doi:https://doi.org/10.1002/hyp.1158, URL https://onlinelibrary.wiley.com/doi/abs/10.1002/hyp.1158, 2003.

Marin, C., Bertoldi, G., Premier, V., Callegari, M., Brida, C., Hürkamp, K., Tschiersch, J., Zebisch, M., and Notarnicola, C.: Use of Sentinel-1 radar observations to evaluate snowmelt dynamics in alpine regions, The Cryosphere, 14, 935–956,

doi:10.5194/tc-14-935-2020, URL https://tc.copernicus.org/articles/14/935/2020/, 2020.

Murfitt, J., Duguay, C. R., Picard, G., and Gunn, G. E.: Investigating the Effect of Lake Ice Properties on Multifrequency Backscatter Using the Snow Microwave Radiative Transfer Model, IEEE Transactions on Geoscience and Remote Sensing, 60, 1–23, doi:10.1109/TGRS.2022.3197109, 2022.

Mätzler, C.: Applications of the interaction of microwaves with the natural snow cover, Remote Sensing Reviews, 2, 259–387, doi:10.1080/02757258709532086, URL https://doi.org/10.1080/02757258709532086, 1987.

Naderpour, R., Schwank, M., Houtz, D., Werner, C., and Matzler, C.: Wideband Backscattering From Alpine Snow Cover: A Full-Season Study, IEEE Transactions on Geoscience and Remote Sensing, PP, 1–15, doi:10.1109/TGRS.2021.3112772, 2021.

Nagler, T., Rott, H., Ripper, E., Bippus, G., and Hetzenecker, M.: Advancements for Snowmelt Monitoring by Means of Sentinel-1 SAR, Remote Sensing, 8, doi:10.3390/rs8040348, URL https://www.mdpi.com/2072-4292/8/4/348, 2016.

Picard, G., Sandells, M., and Löwe, H.: SMRT: an active–passive microwave radiative transfer model for snow with multiple microstructure and scattering formulations (v1.0), Geoscientific Model Development, 11, 2763–2788, doi:10.5194/gmd-11-2763-2018, URL https://gmd.copernicus.org/articles/11/2763/2018/, 2018.

Picard, G., Löwe, H., and Mätzler, C.: Brief communication: A continuous formulation of microwave scattering from fresh snow to bubbly ice from first principles, The Cryosphere, 16, 3861–3866, doi:10.5194/tc-16-3861-2022, URL https://tc.copernicus.org/articles/16/3861/2022/, 2022a.

Picard, G., Löwe, H., Domine, F., Arnaud, L., Larue, F., Favier, V., Le Meur, E., Lefebvre, E., Savarino, J., and Royer, A.: The Microwave Snow Grain Size: A New Concept to Predict Satellite Observations Over Snow-Covered Regions, AGU Advances, 3, e2021AV000 630, doi:https://doi.org/10.1029/2021AV000630, URL https://agupubs.onlinelibrary.wiley.com/doi/abs/10.1029/2021AV000630, e2021AV000630 2021AV000630, 2022b.

Proksch, M., Rutter, N., Fierz, C., and Schneebeli, M.: Intercomparison of snow density measurements: bias, precision, and vertical resolution, The Cryosphere, 10, 371–384, doi:10.5194/tc-10-371-2016, URL https://tc.copernicus.org/articles/10/371/2016/, 2016.

Quéno, L., Fierz, C., van Herwijnen, A., Longridge, D., and Wever, N.: Deep ice layer formation in an alpine snowpack: monitoring and modeling, The Cryosphere, 14, 3449–3464, doi:10.5194/tc-14-3449-2020, URL https://tc.copernicus.org/articles/14/3449/2020/, 2020.

Shi, J. and Dozier, J.: Radar Backscattering Response to Wet Snow, in: [Proceedings] IGARSS '92 International Geoscience and Remote Sensing Symposium, vol. 2, pp. 927–929, doi:10.1109/IGARSS.1992.578299, 1992.

Shi, J. and Dozier, J.: Inferring snow wetness using C-band data from SIR-C's polarimetric synthetic aperture radar, IEEE transactions on geoscience and remote sensing, 33, 905–914, doi:https://doi.org/10.1109/36.406676, 1995.

Sihvola, A.: Mixing Rules with Complex Dielectric Coefficients, Subsurface Sensing Technologies and Applications, 1, 393–415, doi:10.1023/A:1026511515005, URL https://doi.org/10.1023/A:1026511515005, 2000.

Ulaby, F., Long, D., Blackwell, W., Elachi, C., Fung, A., Ruf, C., Sarabandi, K., Zyl, J., and Zebker, H.: Microwave Radar and Radiometric Remote Sensing, 2014.

Viviroli, D. and Weingartner, R.: The hydrological significance of mountains: from regional to global scale, Hydrology and Earth System Sciences, 8, 1017–1030, doi:10.5194/hess-8-1017-2004, URL https://hess.copernicus.org/articles/8/1017/2004/, 2004.

Wever, N., Fierz, C., Mitterer, C., Hirashima, H., and Lehning, M.: Solving Richards Equation for snow improves snowpack meltwater runoff estimations in detailed multi-layer snowpack model, The Cryosphere, 8, 257–274, doi:10.5194/tc-8-257-2014, 2014.

Wever, N., Würzer, S., Fierz, C., and Lehning, M.: Simulating ice layer formation under the presence of preferential flow in layered snowpacks, The Cryosphere, 10, 2731–2744, doi:10.5194/tc-10-2731-2016, URL https://tc.copernicus.org/articles/10/2731/2016/, 2016.